Article

A sensitive electrochemical aptasensor for thrombin detection based on electroactive Co-based metal-organic frameworks with target-triggering NESA strategy

Xia Yang, Jiajia Lv, Zhehan Yang, Ruo Yuan, and Ya-Qin Chai

Anal. Chem., **Just Accepted Manuscript** • DOI: 10.1021/acs.analchem.7b03056 • Publication Date (Web): 11 Oct 2017

A sensitive electrochemical aptasensor for thrombin detection based on electroactive Co-based metal-organic frameworks with target-triggering NESA strategy

Xia Yang[+], Jiajia Lv[+], Zhehan Yang, Ruo Yuan[*], Yaqin Chai[*]

Key Laboratory of Luminescent and Real-Time Analytical Chemistry (Southwest University), Ministry of Education, School of Chemistry and Chemical Engineering, Southwest University, Chongqing 400715, PR China

Abstract:

In this work, an improved target-triggering nicking enzyme signaling amplification (NESA) strategy as signal enhancer has been fabricated to obtain a sensitive electrochemical thrombin (TB) biosensor combined with PtPd NPs decorated electroactive Co-based metal-organic frameworks (Co-MOFs/PtPdNPs) as a redox mediator. Traditionally, in the NESA strategy, only one of the output double strands DNA is available in the next cycle. However, in this work, all of the output DNA involved in the improved NESA strategies could be further employed, resulting in high utilization of output DNA, which further enhanced signal amplification and sensitivity of the biosensor. In addition, the electroactive Co-MOFs were not only used as nanocarriers but also acted as signal labels，avoiding adding extra redox media. Simultaneously, in the presence of H_2O_2, PtPd NPs decorated on the Co-MOFs act as role of Horseradish Peroxidase (HRP) to promote the oxidation of H_2O_2, further

[+] *X. Yang and J. J. Lv contributed equally to this work.*

[*] *Corresponding Author*

E-mail: yuanruo@swu.edu.cn(R.Yuan), yqchai@swu.edu.cn(Y.Q.Chai);

Fax: +86-23-68253172; Tel: +86-23-68252277

promoting the conversion of Co^{2+} to Co^{3+}, leading to electrochemical signal amplification. With such design, the TB biosensor exhibited good sensitivity from 1 pM to 30 nM with a detection limit of 0.32 pM. This new NESA strategy with high utilization of output DNA can supply one efficient approach to improve signal amplification, which also open an avenue for sensitivity enhancement in analytes detection.

Keywords: nicking enzyme signaling amplification, Co-MOFs, aptasensor, thrombin

Introduction

Nicking enzymes can often recognize specific nucleotide sequences with double-stranded DNA and cleave only one of the duplex. With this function, it was employed to design many nicking enzyme signaling amplification (NESA) strategies for detecting different analytes according to the realization of target recycling.[1-6] However, most of NESA strategies reported in previous work generally possessed a drawback of DNA chains waste because one of the obtained DNA cleaved from double-stranded DNA by nicking enzyme was generally useless.[7-10] Thus, a more economical strategy is required to improve the above problem in biosensors.

In addition, metal-organic frameworks (MOFs), as functional porous materials, have significant advantages such as high specific surface area and pore volume, tunable compositions and excellent thermal stability. Therefore, MOFs have been widely applied in gas storage, separation, catalysis and energy storage.[11-18] Among them, the electroactive MOFs, integrating the merits of large surface area as nanocarriers and the redox mediator as signal labels has been emerged to act as an

advanced materials for electrochemical sensors. Moreover, noble-metal nanoparticles with the advantage of fascinating catalytic activity and superior electric conductivity have been wildly employed in biosensors. Especially, nanoalloys of noble-metal nanoparticles, exhibiting enhanced catalytic property due to the synergistic effect, have attracted distinct attention in recent years.[19-23]

In this work, as shown in scheme 1, a sensitive biosensor for thrombin (TB) detection has been developed with the aptamer target-triggering NESA. Firstly, triggered by the recognition between the aptamer and TB, DNA s1 was released and subsequently bond with hairpin DNA (HP1). Nextly, in the presence of nicking endonuclease (Nt.AlwI), DNA s1 would depart from HP1 and be reused to initiate the repeated cycles of hybridization-cleavage. Meanwhile, DNA HP1 would be cleaved into two parts of the output DNA s2 and s2' to unfold the hairpin loop of DNA HP2 supported on the electrode surface and hybridized with it. Then, after the cyclic process, numerous unfolded DNA fragment of HP2 would be generated to further hybridize with DNA HP3, resulting in that a great deal of DNA HP3-conjugated nanomaterials (Co-MOFs/PtPdNPs/HP3) was successfully modified on the biosensor. This fabricated sensor possessed the following merits: Firstly, the nucleotide sequence of HP1 was designed rationally to ensure that the two output DNA s2 and s2' obtained from cleavage of HP1 would own some same nucleotide sequence. Thus all of the output DNA with the specific sequence could be used to hybridize with DNA HP2 for further capturing signal labels, avoiding the waste of DNA chains and obtaining double amount of useful output DNA. Secondly, the prepared Co-MOFs were not

only used as nanocarriers for immobilizing PtPd NPs but also acted as signal labels, avoiding adding redox mediators. Moreover, in the presence of H_2O_2, PtPd NPs decorated on the Co-MOFs act as Horseradish Peroxidase (HRP), which would catalyze the oxidation of H_2O_2 [24-26], further facilitating the conversion of Co^{2+} into Co^{3+} and improving electrochemical signal. With such design, the aptasensor showed good stability, reproducibility, specificity and sensitivity, indicating a promising potential for clinical detection of various proteins with improved sensitivity.

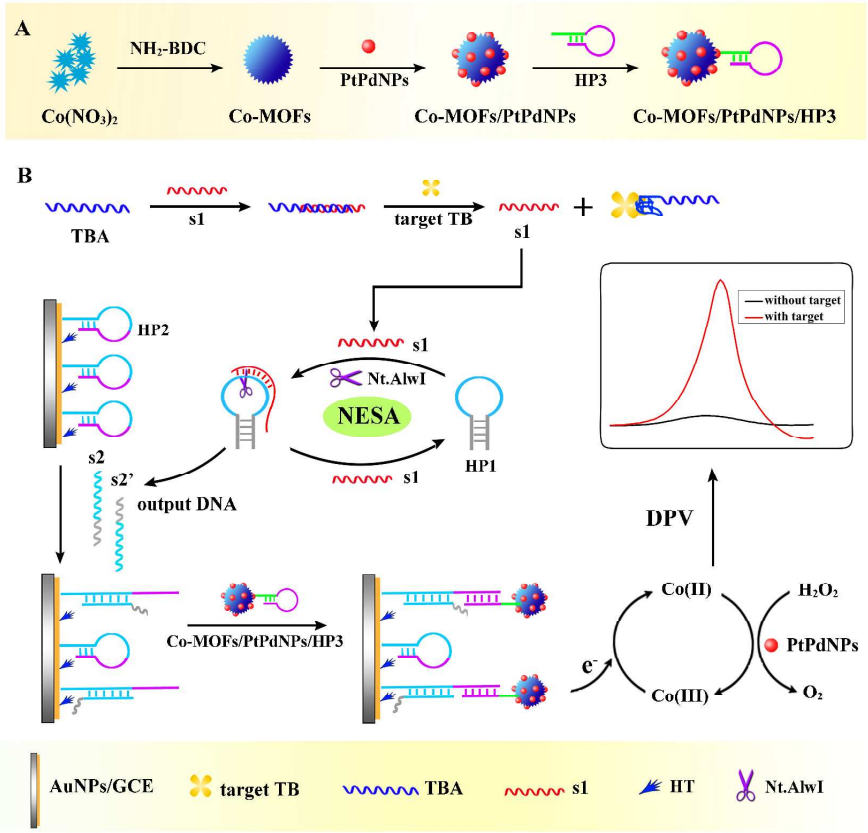

Scheme 1 (A) Preparation of Co-MOFs/PtPdNPs/HP3. (B) The detection principle for TB.

Experimental section

Materials

Thrombin (TB), potassium tetrachloropalladate (K_2PdCl_4), chloroplatinic acid

(H_2PtCl_6), gold chloride ($HAuCl_4$), cetyl trimethyl ammonium bromide (CTAB), and hexanethiol (96%, HT) were bought from Sigma-Aldrich Chemical Co. (St. Louis, MO, U.S.A.). Cobaltous nitrate (Co $(NO_3)_2 \cdot 6H_2O$), 2-amino terephthalic acid (NH_2-BDC) was purchased from KeLong Chemical Co. (Chengdu, China). The nicking enzyme (Nt.AlwI, 10000 U/mL) and 10× NEB buffer (500 mM NaCl, 100 mM Tris-HCl, 100 mM $MgCl_2$, and 10 mM dithiothreitol, pH 7.9) were from the New England Biolabs (Ipswich, U.S.A.). The DNA was obtained from Sangon Biotech Co., Ltd. (Shanghai, China) and the sequences are listed in Table 1:

Table 1. Sequence information of the nucleic acids used in this study

Name	Sequences (5′-3′)
s1	CCA ACC ACA CCA ACC GAT CC
TBA	GGT TGG TGT GGT TGG AGA AGA AGG TGT TTA AGTA
HP1	CCA TTA TCA CGT GGG TGT GGC TGG GAT CGG TTG GTG TGG CTG GGA TCG GTT CAC GTG ATA ATTT
HP2	HS-$(CH_2)_6$-AAC CGA TCC CAG CCA CAC CAC ATG AAC CAA CGT GGC TGG GATA
HP3	HS-$(CH_2)_6$-TTT TCC AAC GTT ATC CCA GCC ACG TTGG

The buffer solutions used in this work are as follows. Tris-HCl buffer (20 mM, pH 7.0) containing NaCl(140 mM), KCl (5 mM) and $MgCl_2$ (1 mM) was used to prepare the oligonucleotide solutions. PBS (0.1 M, pH 7.0) solution with Na_2HPO_4 (10 mM), NaH_2PO_4(10 mM) and $MgCl_2$ (2 mM) was employed to prepare TB solution and used as detection buffer in the experiments. Each hairpin DNA (HP) was heated to 90 ^oC for 10 min and cooled before use.

Apparatus and measurements

Differential pulse voltammetry (DPV) and cyclic voltammetry (CV) were tested by CHI 660D electrochemical workstation. The microstructure of nanomaterials was characterized by scanning electron microscope (SEM, S-4800, Hitachi Instrument, Japan).

Preparation of Co-MOFs

Co-MOFs were prepared through a previous route with some revision.[17] 0.2183 g of Co $(NO_3)_2 \cdot 6H_2O$ and 0.0815 g of NH_2-BDC were mixed into the 4 mL of N,N-Dimethylformamide (DMF). After ultrasonicated for 15 min, the above solution was heated in an oil bath (140 ^oC) for 20 min. The resulting Co-MOFs were obtained by centrifugation. Finally, the collected particles were heated at 60 ^oC for about 6 h for further use.

Preparation of Co-MOFs/PtPd NPs

The Pt-Pd nanoparticles (PtPd NPs) were synthesized according to the reference.[21] First, 200 μL of 2 mM K_2PdCl_4 solution and 40 μL of 10 mM H_2PtCl_6 solution were added into 2 mL of 0.25 mM CTAB solution. Next, 1 mL 0.1 M AA solution was dropped into the above solution under stirring. Then, the obtained mixed solution were transferred into a water bath quickly and heated in 30 ^oC for 5 h. Finally, PtPd NPs were obtained after centrifugation and washed.

Co-MOFs/PtPdNPs were prepared by adding 200 μL of PtPd NPs solution into 1 mL of Co-MOFs solution and stirred for 12 h. The Co-MOFs/PtPdNPs were obtained by centrifugation.

Preparation of Co-MOFs/PtPdNPs/HP3

Firstly, 200 μL of HP3 solution were added into 1 mL Co-MOFs/PtPdNPs and stirred 16 h under 4 ^{o}C. Secondly, the mixed solution was centrifuged and washed. Finally, the obtained product was dispersed in PBS buffer (pH 7.0). The preparation of Co-MOFs/PtPdNPs/HP3 was shown in Scheme 1A.

Fabrication of aptasensor

The detection principle for TB is shown in Scheme 1B. First, TBA and its complementary oligonucleotides 1 (DNA s1) were previously hybridized in equal proportions (20 μL, 2.5 μM) and incubated at 37 ^{o}C for 2 h. Then the obtained complex was incubated in 20 μL different concentrations of TB at 37 ^{o}C for 2 h. When the biosensor was incubated with different concentration of TB, different amount of single-stranded DNA s1 was released from the TBA/S1 hybrids in the process.

The recycle process was performed as follows: the released DNA s1 solution (20 μL), HP1 solution (2 μM, 10 μL) and NEB buffer (10×, 10 μL) were mixed and incubated at 37 ^{o}C for 45 min. Then, 5 μL 2 U/μL Nt.AlWI was added and incubated at 37 ^{o}C for 2 h. After incubation, the obtained mixtures were heated at 80 ^{o}C for 20 min to terminate the reaction.

Firstly, the cleaned glassy carbon electrode GCE was dipped into $HAuCl_4$ solution (1 *wt* %) and electrodeposited at -0.2 V for 30 seconds to obtain gold nanoparticles (AuNPs) layer. After washed, the GCE was incubated with 20 μL HP2 solution (2 μM) for about 16 h at room temperature. Then, 20 μL HT solution (1.0 mM) was dropped to block the nonspecific combining sites. Subsequently, 20 μL

resultant output DNA s2 and s2' was dropped onto the electrode and incubated for 2 h at 37 ^{o}C to unfold the HP2. After that, the electrode was washed and incubated with 20 μL of the Co-MOFs/PtPdNPs/HP3 for 2 h.

Results and discussion

Characteristics of Co-MOFs

Figure 1A is the SEM image of Co-MOFs with flower-like structures. After PtPd NPs was coated on the Co-MOFs (Figure 1B), intensive highlights represented PtPd NPs could be clearly observed on the surface of Co-MOFs sphere, revealing that the PtPd NPs were successfully captured on Co-MOFs.

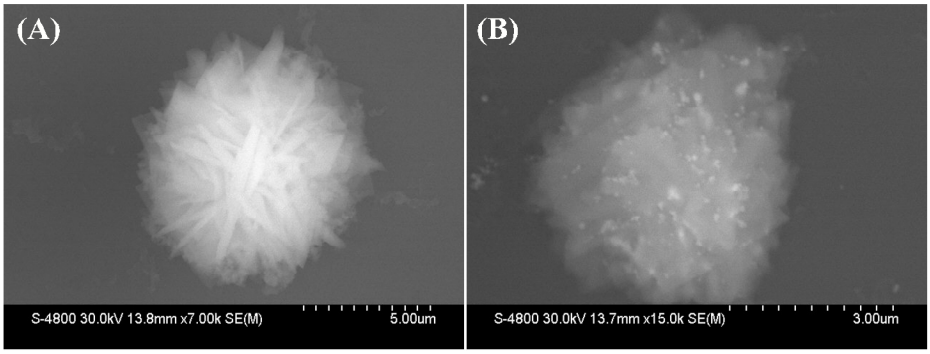

Figure 1 SEM images of (A) flower-like Co-MOFs nanostructures and (B) Co-MOFs/PtPdNPs nanocomposites.

CV *of the aptasensor*

To characterize the electrochemical properties of the aptasensor, CV was employed to follow the stepwise modified process. CVs was tested in 5 mM $[Fe(CN)_6]^{3-/4-}$ solution at 100 mV/s (Figure 2). Bare GCE (curve a) showed smaller current than the AuNPs/GCE (curve b), which because the better conductive ability of AuNPs. Due to that the aptamer can severely increase the steric hindrance, the current

dramatically decreased after HP2 was assembled onto the electrode surface (curve c), demonstrating the successful modification of HP2. Then the current decreased further (curve d) after the electrode was incubated with HT. This is due to that the HT makes a blockage of electronic transportation. Additionally, when the mixtures containing NEB buffer and output DNA s2/s2' was on the electrode, the peak current decreased (curve e), which is due to that the specific binding between DNA HP2 and DNA s2/s2' would retard the electron transfer.

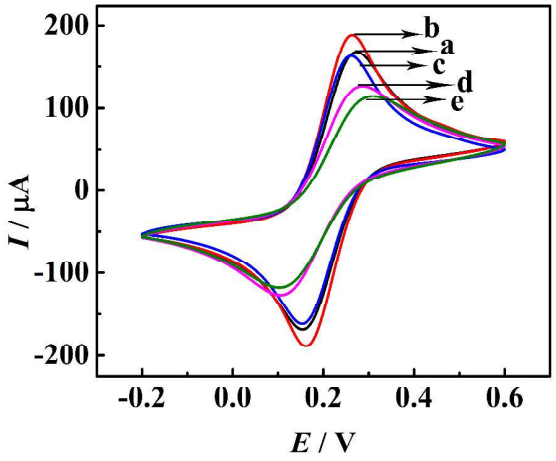

Figure 2 CVs of the different modified electrode at 100 mV/s in 5 mM $[Fe(CN)_6]^{3-/4-}$ solution : (a) bare GCE, (b) AuNPs/GCE, (c) HP2/AuNPs/GCE (d) HT/ HP2/AuNPs/GCE, (e) s2 (s2')/HT/HP2/AuNPs/GCE.

Optimization of detection conditions

The test conditions such as the concentration of H_2O_2, the pH of solution and the reaction time of recycle process were investigated by the aptasensor with 10 nM TB as a model. Firstly, the concentration of H_2O_2 in testing buffer solution plays an important role in this strategy. To investigate the effect of H_2O_2 concentration, the aptasensor was detected in PBS solution (pH 7.0) with different concentration of

H_2O_2 (from 1.69 mM to 3.68 mM). In Figure 3A, with the concentration of H_2O_2 increased, the peak current increased and become stable at 3.21 mM, suggesting the highest electrocatalytic efficiency at this point. Therefore, 3.21 mM of H_2O_2 was selected throughout the whole experiment.

In this work, the fabricated aptasensor was detected in PBS buffer with different pH value. In Figure 3B, from 5.0 to 7.0, the current increased with the pH value increased firstly and then decreased after the pH value was larger than 7.0. Therefore, the value of 7.0 for the working buffer was adopted for the investigation.

The reaction time of recycle process was studied from 20 min to 140 min. From the results indicated in Figure 3C, we can see the peak current increased when the recycle time achieved to 120 min, where a maximum current was obtained. After 120 min, the peak current has no obvious change. Therefore, the optimal reaction time of recycle process was chosen as 120 min.

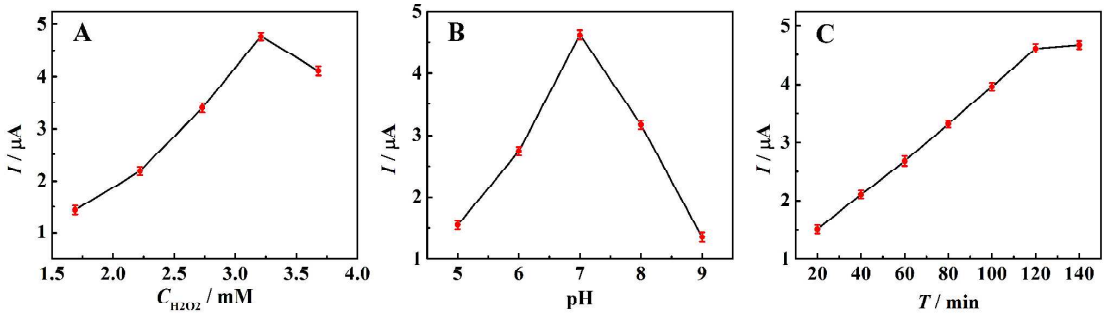

Figure 3 Optimization of (A) the concentration of H_2O_2 and (B) the pH value. (C) the nicking time.

Calibration curves of the aptasensor

In optimized experiment conditions, the aptasensors were incubated in different concentrations of TB. In Figure 4, it could be seen that with no target of TB, the DPV

current response was very low, indicating the ignorable unspecific binding. Furthermore, the peak current showed a linear range with logarithm of TB concentration from 1 pM to 30 nM. The linear equation was $I = 0.8209 \lg c + 4.207$ ($R = 0.9912$) and the detection limit was 0.32 pM. And the error bars were calculated by three detections. In comparison with references (Table 2), this aptasensor showed better detection limit for TB detection.

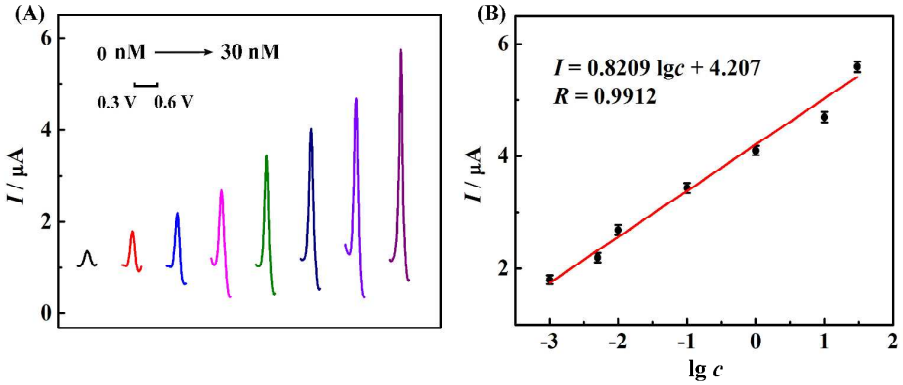

Figure 4 (A) DPV curves (0.3 V~0.6 V) of the aptasensor after incubated with different concentrations of TB. (B) Calibration plots of peak current *vs.* the logarithm of the TB concentration

Table 2. Comparison of other works for thrombin detection.

Analytical method	Linear range	Detection limit	Reference
Different pulse Voltammetry	0.1-10 nM	0.07 nM	27
Different pulse Voltammetry	0.1-25 nM	0.02 nM	28
Different pulse Voltammetry	0.01-50 nM	5.6 pM	29
Different pulse Voltammetry	0.001-30 nM	0.32 pM	This work

Selectivity, reproducibility and stability

Some interferences including hemoglobin (Hb), carcinoembryonic antigen (CEA), bovine serum albumin (BSA) and human IgG were incubated under the same experiment conditions to test the aptasensor. In Figure 5, when Hb, CEA, BSA and

human IgG (each concentration was 100 nM) was used to replace TB, respectively, the changes of the current were negligible. While the electrode was incubated in a mixed solution which contained the target TB and the above four interferences (each concentration were 10 nM), high current response are obtained and the value is same as that with only TB (10 nM), demonstrating the aptasensor had good selectivity.

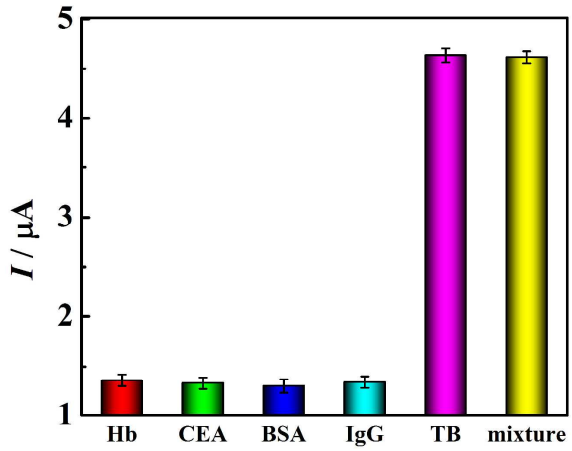

Figure 5 Selectivity of the proposed TB aptasensor.

The reproducibility of the aptasensor was studied as follows. In the same condition, four batches of the aptasensors were employed to detect 10 nM TB. And these four aptasensors exhibited similar current response with a relative standard deviation (RSD) of 3.92%. Furthermore, 10 nM TB was tested by one aptasensor for four times with RSD of 4.26%. The results demonstrated a good reproducibility of the aptasensor.

The aptasensor was kept at 4 ^{o}C and tested each day. After stored for 15 days, the electrochemical signal maintained 92.6% of its original current response, showing that the prepared aptasensor had satisfactory stability.

Application of the aptasensor

Different amount of TB were added into human serum samples (10-fold-diluted, obtained from Ninth People's Hospital of Chongqing, China). Then we use the proposed aptasensor to test the concentration of TB in the samples. As shown in Table 3, the recovery was from 90.8% to 106.4%, while the RSD was in the range of 2.8% to 5.1%, respectively. This showed that the aptasensor can be potentially applied for TB detection.

Table 3. Detection of TB added in human serum (n = 3)

Serum samples	Added TB/nM	Founded TB/nM	RSD/%	Recovery/%
1	5.0×10^{-3}	4.56×10^{-3}	4.3	91.2
2	1.0×10^{-2}	9.47×10^{-3}	2.8	94.7
3	5.0×10^{-2}	5.32×10^{-2}	3.7	106.4
4	0.5	0.51	3.4	102.0
5	5.0	4.54	5.1	90.8

Conclusion

In this work, we designed a sensitive aptasensor for TB detection employing the improved NESA strategies and Co-MOFs/PtPdNPs nanomaterials. This fabricated sensor possesses these following advantages: Firstly, the designed NESA strategies could realize signal amplification through the target recycling and solve the problem of DNA chain waste in traditional NESA strategies. Secondly, the prepared flower-like Co-MOFs with large surface area were applied as nanocarriers and signal labels, avoiding adding redox media. Finally, PtPd NPs can catalyze the oxidation of H_2O_2 for further signal amplification. With such design, this aptasensor has good sensitivity, demonstrating a promising potential approach for sensitivity enhancement

in clinical application.

5. Acknowledgements

The authors are grateful for the National Natural Science Foundation of China (21675129, 21575116 and 51473136), the Fundamental Research Funds for the Central Universities (XDJK2016E055, XDJK2015C099, SWU114079), China Postdoctoral Science Foundation (2015M572427, 2016T90827) and Chongqing Postdoctoral Research Project (xm2015019).

References

1. Zhang, K.; Wang, K., Zhu, X., Zhang, J.; Xu, L.; Huang, B.; Xie, M. H. *Chem. Commun.* **2014**, *50*, 180-182.

2. Zhang, Q.; Chen, F.; Xu, F.; Zhao, Y. X.; Fan, C. H. *Anal. Chem*. **2014**, *86*, 8098-8105.

3. Huang, J.; Li, X. Y.; Du, Y. C.; Zhang, L. N.; Liu, K. K.; Zhu, L. N.; Kong, D. M. *Biosens. Bioelectron.* **2017**, *91*, 417-423.

4. Yao, G. H.; Liang, R. P.; Yu, X. D.; Huang, C. F.; Zhang, L.; Qiu, J. D. *Anal. Chem.* **2015**, *87*, 929-936.

5. Wang, X. Z.; Hou, T.; Dong, S. S.; Liu, X. J.; Li, F. *Biosens. Bioelectron.* **2016**, *77*, 644-649.

6. Li, L.; Wang, Q.; Feng, J.; Tong, L. L.; Tang, B. *Anal. Chem.* **2014**, *86*, 5101-5107.

7. Wang, G. L.; Fang, X.; Wu, X. M.; Hu, X. L.; Li, Z. J. *Biosens. Bioelectron.* **2016**, *81*, 214-220.

8. Liu, X. J.; Chen, M. Q.; Hou, T.; Wang, X. Z.; Liu S. F.; Li, F. *Biosens. Bioelectron.* **2014**, *54*, 598-602.

9. Yao, G. H.; Liang, R. P.; Yu, X. D.; Huang, C. F.; Zhang, L.; Qiu, J. D. *Anal. Chem.* **2015**, *87*, 929-936.

10. Yang, J. M.; Dou, B. T.; Yuan, R.; Xiang, Y. *Anal. Chem.* **2016**, *88*, 8218-8223.

11. Zhu, Q. L.; Xu, Q. *Chem. Soc. Rev.* **2014**, *43*, 5468-5512.

12. Lv, Y. Y.; Wang, Y. T.; Li, H. L.; Lin, Y.; Jiang, Z. Y.; Xie, Z. X.; Kuang, Q.; Zheng, L. S. *ACS Appl. Mater. Interfaces* **2015**, *7*, 13604-13611.

13. Liu, L. L.; Song, Y. B.; Chong, H. B.; Yang, S.; Xiang, J.; Jin, S.; Kang, X.; Zhang, J.; Yu, H. Z.; Zhu, M. Z. *Nanoscale* **2016**, *8*, 1407-1412.

14. Lee, H. J.; We, J. H.; Kim, J. O.; Kim, D. Y.; Cha, W. H.; Lee, E. J.; Sohn, J. W.; Oh, M. H. *Angew. Chem. Int. Ed.* **2015**, *54*, 1-6.

15. Chughtai, A. H.; Ahmad, N.; Youns, H. A.; Laypkov, A.; Verpoort, F. *Chem. Soc. Rev.* **2015**, *44*, 6804-6849.

16. Li, S. Z.; Huo, F. W. *Nanoscale* **2015**, *7*, 7482-7501.

17. Xia, W.; Mahmood, A.; Zou, R. Q.; Xu, Q. *Chem. Soc. Rev.* **2015**, *8*, 1837-1866.

18. Cui, L.; Wu, J.; Li, J.; Ju, H. X. *Anal. Chem.* **2015**, *87*, 10635-10641.

19. Sun, Y. F.; Li, J. H.; Cui, L.; Hua, B.; Cui, S. H.; Li, J.; Luo, J. L. *Nanoscale* **2017**, *9*, 947-947.

20. Li, P. Y.; Li, F. S.; Deng, G. D.; Guo, X. D.; Liu, H. Y.; Jiang, W.; Wang, T. H. *Chem. Commun.* **2016**, *52*, 2996-2999.

21. He, W. W.; Wu, X. C.; Liu, J. B.; Hu, X. N.; Zhang, K.; Hou, S.; Zhou, W. Y.; Xie, S. S. *Chem. Mater.* **2010**, *22*, 2988-2994.

22. Darabdhara, G.; Boruah, P. K.; Borthakur, P.; Hussain, N.; Das, M. R.; Ahamad, T.; Alshehri, S. M.; Malgras, V.; Wu, K. C. W.; Yamauchi, Y. *Nanoscale* **2016**, *8*, 19174-19175.

23. Fu, S. F.; Zhu, C. Z.; Shi, Q. R.; Xia, H. B.; Du, D.; Lin, Y. H. *Nanoscale* **2016**, *8*, 5076-5081.

24. Xu, W. J.; Yi, H. Y.; Yuan, Y. L.; Jing, P.; Chai, Y. Q.; Yuan, R. *Biosens. Bioelectron.* **2015**, *64*, 423-428.

25. Wu, X. Y.; Chai, Y. Q.; Zhang, P.; Yuan, R. *ACS Appl. Mater. Interfaces* **2015**, *7*, 713-720.

26. Cui, L.; Wu, J.; Li, J.; Ju, H. X. *Anal. Chem.* **2015**, *87*, 10635-10641.

27. Ahour, F.; Ahsani, M. K. *Biosens. Bioelectron.* **2016,** *86*, 764-769.

28. Zheng, Y. N.; Yuan, Y. L.; Chai, Y. Q.; Yuan, R. *Biosens. Bioelectron.* **2015**, *66*, 585-589.

29. Yang, J. M.; Dou, B. T.; Yuan, R.; Xiang, Y. *Anal. Chem.* **2016**, *88*, 8218-8223.

Table of contents